Journal of Alloys and Compounds 507 (2010) 207–214

Contents lists available at ScienceDirect

Journal of Alloys and Compounds

journal homepage: www.elsevier.com/locate/jallcom

Deformation homogeneity in accumulative back extrusion processing of AZ31 magnesium alloy

S.M. Fatemi-Varzaneh*, A. Zarei-Hanzaki, M. Naderi, Ali A. Roostaei

School of Metallurgical and Materials Engineering, University of Tehran, Tehran, Iran

ARTICLE INFO

Article history:
Received 27 May 2010
Received in revised form 17 July 2010
Accepted 21 July 2010
Available online 30 July 2010

Keywords:
SPD
ABE
AZ31 alloy
Strain homogeneity

ABSTRACT

The ultra-fine grained materials produced by severe plastic deformation (SPD) methods have been widely investigated in the last decades due to the enhanced material properties such as improved tensile strength, hardness, toughness, fatigue life, and the optical and electrical related properties. The microstructure and mechanical properties of the deformed materials are strongly dependent on the amount and the homogeneity of strain achieved during the SPD processes. Accumulative back extrusion (ABE) method is a novel severe plastic deformation (SPD) technique which has been recently developed for fabrication of bulk ultra-fine structured materials. The knowledge of strain distribution and deformation behavior during ABE processing may assist the better understanding of the whole process. Therefore the present work has been conducted to examine the strain distribution and deformation behavior during ABE process through applying 3D finite element simulations with Abaqus/Explicit for different stages of deformation. In order to validate the simulation results, a grid method assessment was employed. The results demonstrated that a homogenous equivalent plastic strain of 4–5 has been gained after applying one pass ABE. In addition the results indicate that the distribution of normal strain is inhomogeneous. The microstructural observations have revealed a proper structural homogeneity after completion of an ABE cycle.

© 2010 Elsevier B.V. All rights reserved.

1. Introduction

In recent years, several methods of severe plastic deformation (SPD) have been under focus of numerous investigations due to the superior mechanical and physical properties of achieved ultra-fine grained materials [1]. In fact a very large strain is adapted to generate an ultra-fine grain material. In addition the homogeneity of this grain refinement plays the key role in the superior mechanical properties of SPD processed materials [2]. As the microstructure and mechanical properties of any deformed material are directly related to the amount and the mode of applied plastic deformation, the understanding of their associated phenomena is highly necessitated.

The distribution of equivalent plastic strain and stress developed in equal channel angular pressing (ECAP) has been already analyzed [3–6]. These were performed through considering the different die angles and friction conditions. The latter was applied on different materials such as Al-1100 [3], Al-6061 [4,5] and Al-3103 [6] with the aim of determining the deformation behavior and strain homogeneity. The direct observation of shear deformation has been also brought in reality through ECAP of pure aluminum with a 90° die angle. In the case of ECAP deformation, the results showed that the materials on the outer side of the extrusion channel undergone more severe plastic deformation compared to those on the inner side of the extrusion channel [5]. Moreover, the study of effective strain variation across the width at the centre of the ECAP specimens indicated that the strain homogeneity was higher for $\varphi = 90°$ compared to the other channel angles [3]. Since the amount of deformation which can be applied during any single pass ECAP is limited, preserving the desired level of homogeneity in the related cross-section is difficult. To overcome this restriction and improve the efficiency of the ECAP, a new method known as twist channel angular pressing (TCAP) was introduced [7]. The latter (a single pass TCAP) could ensure the higher strain values with more homogeneity across the cross-section.

In the case of other SPD methods some efforts have been provided to analyze the deformation behavior of material during high pressure torsion [8], differential speed rolling [9], and multiple forging [10].

Recently a new SPD method based on an accumulative back extrusion (ABE) processing has been innovated and introduced [11]. The schematic representation of ABE process is given in Fig. 1. In comparison to the other SPD processes, ABE possesses many advantages, such as lower required load, and no need of interpass operation and reheating. As was well demonstrated, ABE

* Corresponding author at: Hot Deformation Lab, Metallurgy and Materials Engineering, North Karegar, Tehran, Iran. Tel.: +98 2161114167; fax: +98 2188006076.
E-mail address: mfatemi@ut.ac.ir (S.M. Fatemi-Varzaneh).

0925-8388/$ – see front matter © 2010 Elsevier B.V. All rights reserved.
doi:10.1016/j.jallcom.2010.07.157

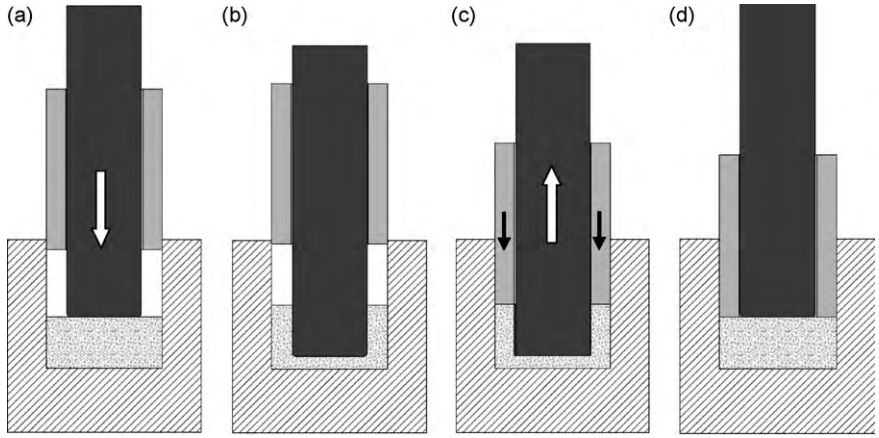

Fig. 1. The schematic illustration of ABE which shows a single pass processing (each pass includes two steps deformation): (a) initial state, (b) step one, back extrusion, (c) step two, compression back, (d) end of process [10].

process may be considered as a powerful technique to achieve an outstanding grain refining in AZ31 magnesium alloy down to sub-micrometer size [12]. However to empower this marvelous finding, a reevaluation of the process should be performed using the efficiency and capability of the finite element modeling (FEM).

The present work has been conducted to investigate the deformation homogeneity in the ABE processed material through finite element simulation. In order to validate the simulation results, a special grid method was employed to directly trace the deformation pattern. The proper microstructural observations were also executed on deformed material to analyze the microstructural evolution, in particular its homogeneity, during ABE process.

2. Experimental and simulation procedure

The principle of accumulative back extrusion processing was described elsewhere [11]. A hot rolled AZ31 wrought magnesium alloy has been employed as experimental and simulation alloy. The cylindrical testing work-pieces were machined in the sizes of φ18 mm × 8 mm. The MoS_2 spray was used to reduce the friction between the work piece and the tools surfaces. The specimens were cut into two halves before applying the ABE to directly monitor the strain evolutions during processing. The square grids with dimension of 1 mm were electro-etched on the face of one-half. A clear strain deformation pattern could be observed through employing this special technique. The experiments were conducted at 300 °C by a ram speed of 10 mm/min. The microstructural investigations were done through common metallographical methods.

The 3D FEM simulations have been carried out to analyze the overall behavior of the specimen in the die. In this way the total equivalent plastic strain (EPS), normal strain (NS) and Von-Mises stress could be evaluated. The commercial finite element code Abaqus/Explicit was used to perform all the simulations. An eight-node bilinear plane strain hexahedral (C3D8R) element was employed for the parts. The initial element mesh contains 44,580 elements. To accommodate large strains during simulations the adaptive meshing (automatic remeshing) was utilized. The arbitrary Lagrangian Eulerian (ALE) adaptive meshing, would maintain a high-quality mesh under severe material deformation by allowing the mesh to move independently with respect to the underlying material. In addition it maintains a topologically similar mesh throughout the analysis (i.e., elements are not created or destroyed). A similar cylindrical shape sample was also considered for the simulations. Von-Mises yield criterion was adapted for the simulation sample. The frictional conditions at the punch-specimen and die-specimen interfaces are described by Coulomb friction model. The sticking friction condition which may occur at some interfaces during the process would alter the temperature and material properties in this region. In this analysis for the sake of simplicity, the sliding friction model was hypothesized. The sliding friction coefficient (η) was assumed to be 0.15. The die and the punch were modeled with analytical rigid elements. The friction coefficient (m) was assumed to be 0.15. All simulations were performed with a speed of 10 mm/min. In order to run the simulations, the mechanical properties of AZ31 alloy which were obtained through hot compression tests [13], and the mechanical properties of a hot worked steel to model the punch have been taken into account. The physical properties of the experimental alloy which were utilized for the simulations are given in Table 1. The strategy of different point evaluations was selected to examine the evolution of strain and stress in whole sample.

In a quasi-static analysis, it is advantageous to reduce the computational cost by either speeding up the simulation or by scaling the material mass. At the same time, it is crucial that the dynamic effects in the analysis do not influence the stability of the solution. In each circumstance, the value of the kinetic energy should not exceed a small fraction of the value of the strain energy. In this analysis, by monitoring kinetic energy it was made certain that the ratio of kinetic energy to internal energy does not get too large.

3. Results and discussion

3.1. Deformation behavior

Fig. 2 displays the EPS contours of the deformed sample during ABE steps. As is seen the results are presented in two dimensions and to facilitate the demonstration of the plastic strain contours in the sample, the dies and guides are not included. As is observed the regions along the top areas are severely deformed. This severe deformation is not seen at the centre and the regions right below the punch. The distribution of effective strain (or EPS) is inhomogeneous in the early stages of deformation, but it goes to be more homogenized by approaching to the final stages. This can be appreciated through the color variations in Fig. 2. In the step one, the strain inhomogeneity in the bottom areas is attributed to the difficulties of material flow in this region. In addition the achieved EPS in regions close to the die bottom and the wall is lower in comparison to the other areas. However this is higher in the regions of the channel between the die and the inner punch.

In order to clarify the state of dominant stress–strain behavior during the ABE process, it is necessary to follow the material flow paths. This would be done through dividing the deformation into different events as are fallows. The deformation may initially start in the region above the center line (i.e., the materials close to the head of the inner punch). The material flows toward the gap between the inner punch and the die via shear deformation (Fig. 2). In addition the material flow is mainly conducted through a bent channel (Figs. 2 and 3). The material outside the channel affects by normal strain rather than shear strain (see Fig. 3). It is worth mentioning that the locus of deformation channel moves down as the inner punch proceeds. The tie regions between punch edge and

Table 1
The physical properties of AZ31 experimental alloy.

Material parameter	Value
Young's modulus (E)	41E9 Pa
Poisson's ration (ν)	0.35
Density (ρ)	1.78 g/cm^3
Friction coefficient (η)	0.15

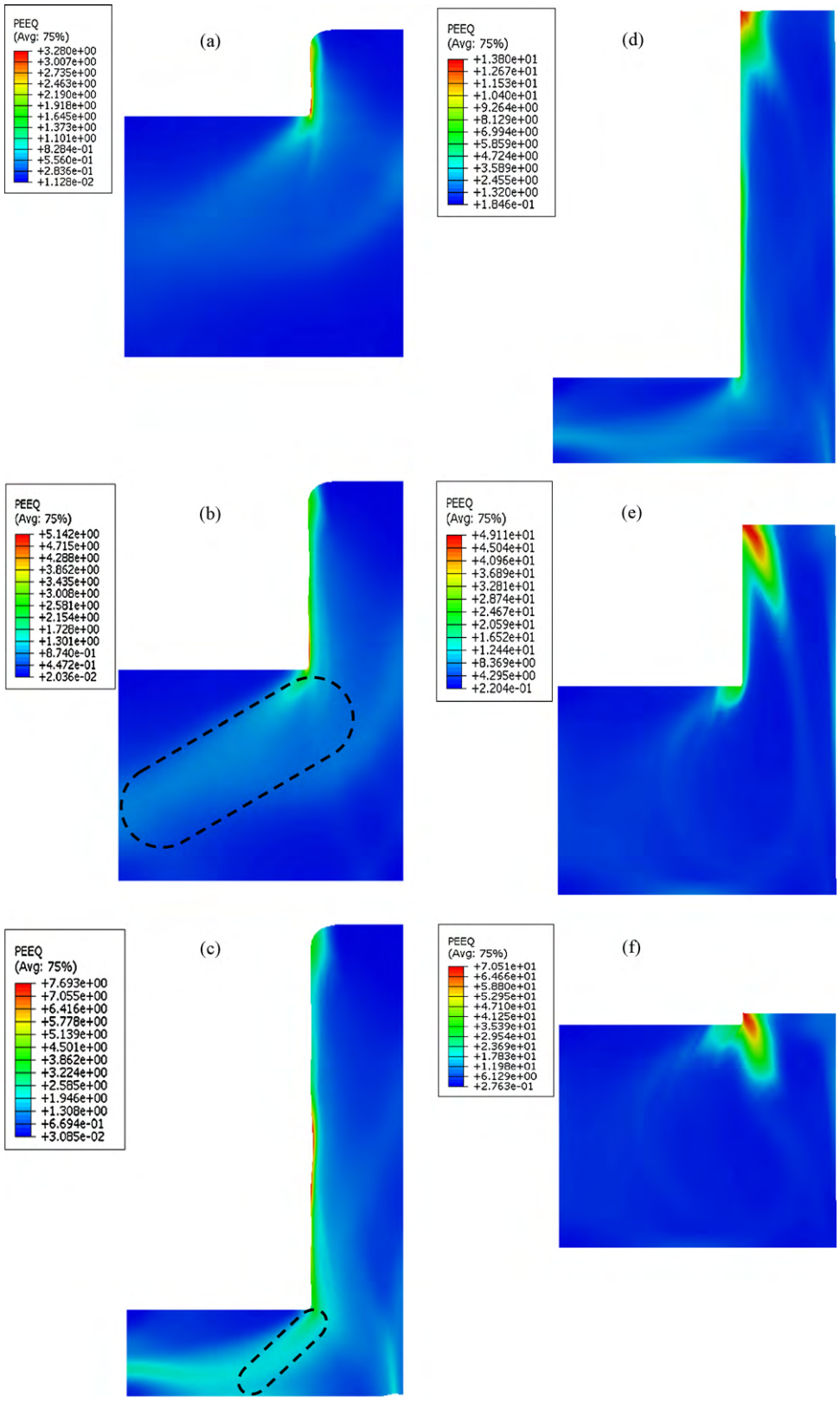

Fig. 2. The EPS contours of the experimental alloy at different ABE stages (a, b, c step one and d, e, f step two).

bottom center show the areas of intense strain. As the deformation approach to the end of step one, the dead zone which was formed under the punch head, shears off gradually toward the inner punch edges. It should be noted that the workpiece at the end of step one is a cup-shaped specimen. The maximum and minimum equivalent plastic strains are achieved at inner side of cup wall and the cup bottom (below the punch head), respectively. As the second step of ABE (i.e., compressing back) proceeds a similar deformation route is inversely introduced. The NS contours in Fig. 3 depict the flow back of material to the initial shape. As is seen a similar pattern to

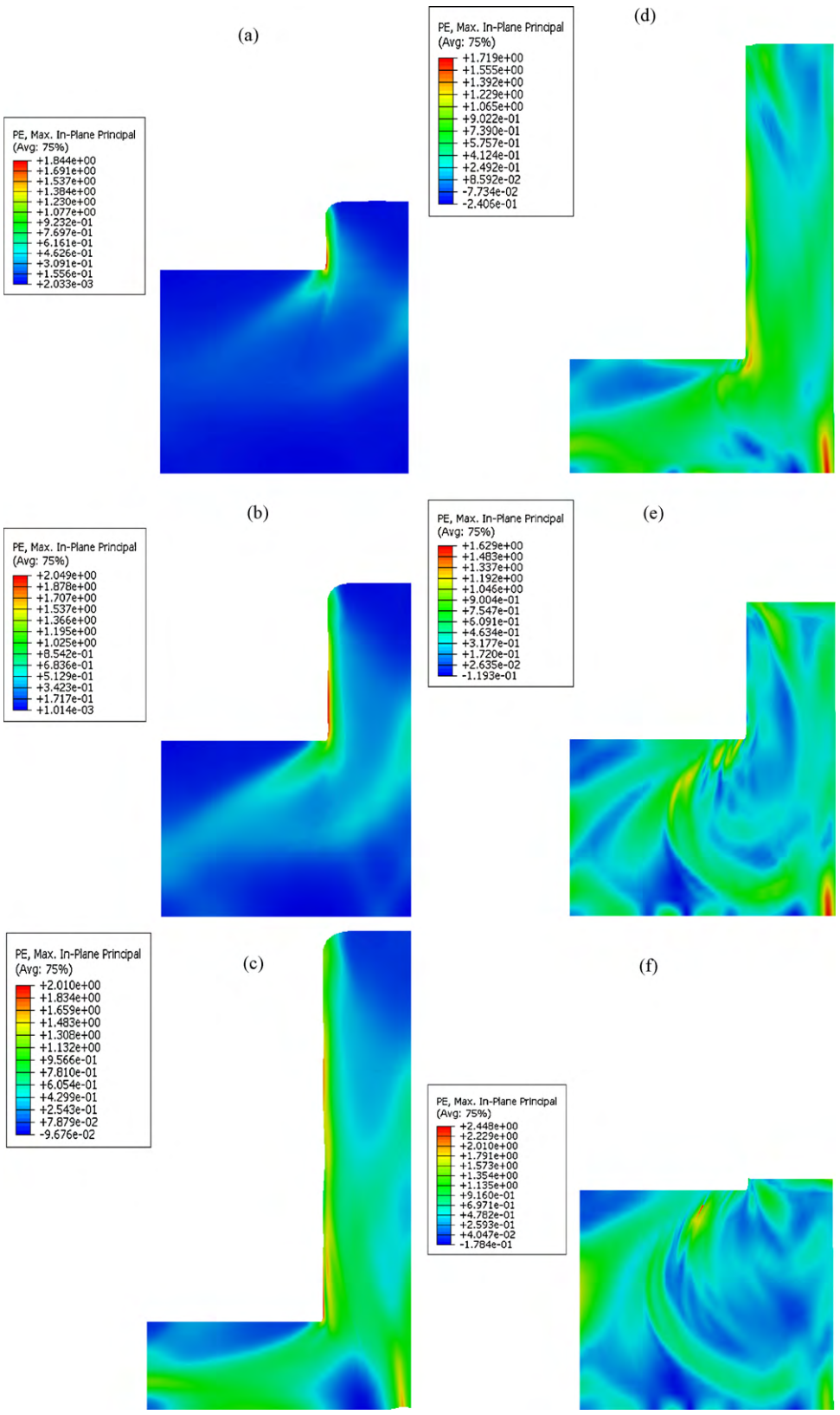

Fig. 3. The NS contours of the experimental alloy at different ABE stages (a, b, c step one and d, e, f step two).

EPS contours has been also developed for NS distribution at the end of step one.

The calculated strain distributions during step two show that the deformation penetration may effectively cover the whole sample (Figs. 2 and 3d–f). As is seen the NS is heterogeneously distributed at the end of process. The EPS (effective strain) distribution is more uniform in the major part of the sample (Fig. 2f). However as is seen in Fig. 2f a few areas of inhomogeneity including high strain values

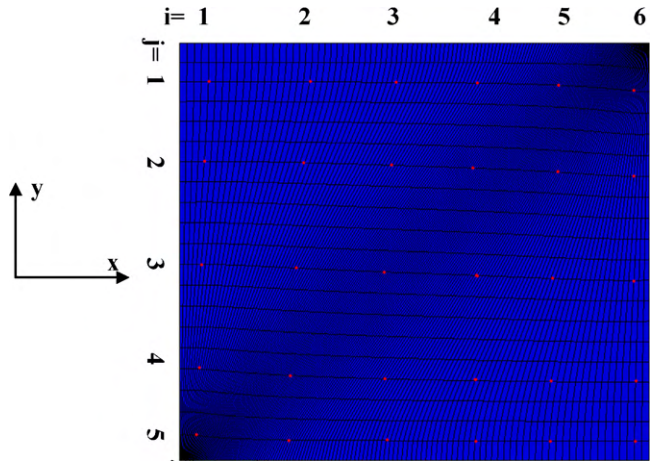

Fig. 4. The selected nodes in one-half of the specimen cross-section.

may also be realized. The EPS in the most regions is found to be in the range of 4–5. Such a high amount of EPS has not been already reported at the end of first pass of any SPD processes. For C-shape equal channel reciprocating extrusion (CECRE) [14] and TCAP [7], as the newly developed SPD techniques, the values of 2.74 and 2.30 were estimated, respectively. The analysis of material flow pattern and the state of strain revealed the zone of more severe plastic deformation (Fig. 2). As is highlighted in Fig. 2b and f, this narrow zone (thick plate-like in two-dimensional patterns) is positioned inclined with respect to the punch tip. The authors consider this region as a pronounced shear plane. According to the aforementioned observations the strain homogeneity in the ABE is mainly achieved by passing the material across this shear plane.

As is well established the most of flow defects which appear in such a forming process is attributed to the material flow restriction ending to a dead metal zone formation. Consequently it is crucial to control the material flow to eliminate this zone [15]. In ABE process, as the outer punch is being pushed down, the inner punch is loosely being lift up by undergoing material flow. This controls the material flow thereby suppressing defect formation.

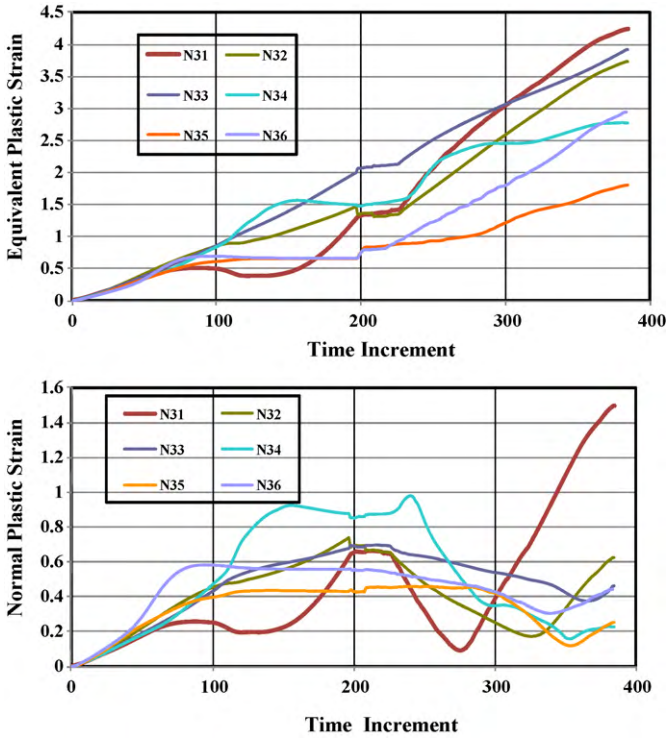

Fig. 5. The variations of plastic strains along the specimen width at various times during the ABE deformation process for nodes N3*j*, *j* = 1–6.

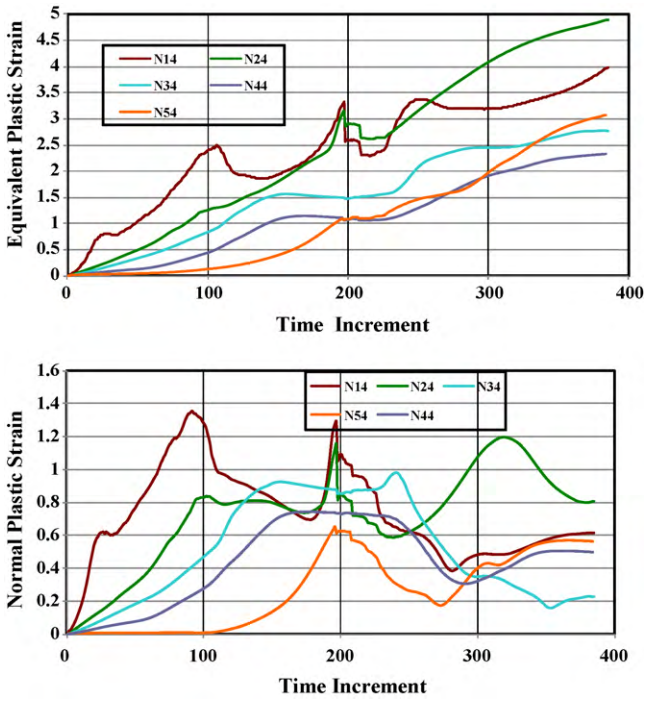

Fig. 6. The variations of plastic strains along the specimen height in various times during the ABE deformation process for nodes Ni4, *i* = 1–5.

3.2. Plastic strain

To quantify the strain homogeneity in ABE processing the equivalent and normal plastic strain (along the deformation axis) were analyzed across the cross-section. As is illustrated in Fig. 4, 30 nodes were considered to follow the overall view of the material flow. Two typical sets of nodes (i.e., N3*j*, *j* = 1–6, and Ni4, *i* = 1–5) were traced to represent the different deformation zones. The deformation history developed along *X*- and *Y*-axis (i.e. width and height of sample) is depicted in Figs. 5 and 6, respectively. As is understood from Fig. 5, almost all of the nodes along the width (*X*-axis) start to be concurrently deformed. In the case of EPS, the strain accumulation in nodes takes a similar incremental trend in all regions during both steps of ABE. The normal strain however decreases after the process reaches the mid-time situation where step two is being applied. This implies that the share of normal strain in EPS decreases but the role of shear strain is pronounced in step two. The maximum values of 1.5 and 4.2 are achieved for the NS and EPS, respectively; both of which are almost produced at the center of cross-section (N31). The EPS and NS variations along the *Y*-axis follow a similar trend to that of *X*-axis. However, more heterogeneity may be realized in strain values experienced along *Y*-axis. According to Fig. 6, the closer the regions to the head of inner punch, the faster the deformation is undergone. The maximum values of 0.8 and 4.8 are achieved for the NS and EPS in this case, respectively. These are achieved in the region below the surface at the vicinity of the inner punch edge (N42).

3.3. Comparison of FEM and experimental results

The deformation behavior was examined considering the distortions of the grids plotted on the cross-section by geometrical

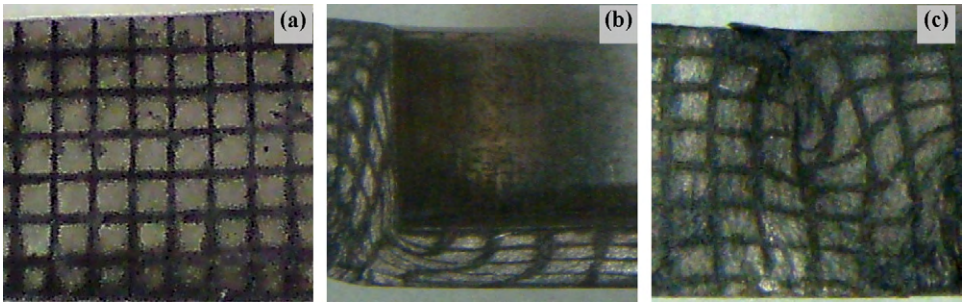

Fig. 7. (a) The deformation mesh at initial state; and the deformed mesh at the end of (b) step one, and (c) step two of ABE process.

measurement. The deformed work-pieces are shown in Fig. 7. The grids have been gradually deformed during step one (i.e., throughout back extrusion step). However the distorted grids have been gradually gained their initial shape during the second step. To verify the simulation results a comparison was conducted between the normal strains calculated through simulation method and those of measured ones by grid method. The normal strains were measured along *Y*-axis for a given grid. The developed normal strains at two different processing conditions (mid-time and end of process) as well as the measured ones are plotted against the distance from the bottom of workpiece in Fig. 8. To evaluate the strain homogeneity, the Ni2 nodes (close to the center line) and Ni4 (close to the surface) were traced. The verification results indicate that the material flow pattern is qualitatively well similar to the simulated one.

The obtained microstructures after single pass ABE processing are shown in Fig. 9. As is seen a homogenous grain refinement has been achieved. Although the EPS estimation (Fig. 2f) denotes a kind of heterogeneity in some small regions of high EPS values (20–40), but suitable strain homogeneity is realized at the end of deformation (Fig. 2f). In addition a clear distinction may not be realized between the regions of more severely strained than that of slighter ones. This is attributed to the saturation of the potential nucleation sites in the microstructure. In the other words, as has been already reported for grain refinement during SPD process, there is a minimum dislocation density gradient below which the grain refinement is highly sluggish [16].

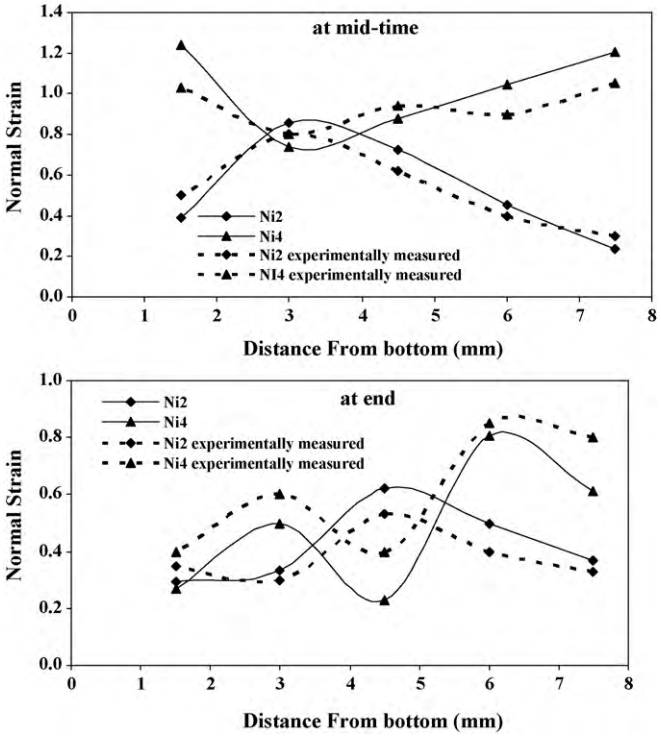

Fig. 8. The profiles of equivalent plastic strain along the Ni2 and Ni4 nodes of the work piece at the (a) middle and (b) end of total deformation times.

3.4. Von-Mises stress profile

As is well established, analyzing the effective stress contours in the deformation zone may generate some information about shear deformation and plastic zones [3]. Fig. 10 represents the effective stress contours for a range of deformation steps. Inadequate plastic zones indicate the regions where were not subjected to the plastic deformation. This in turn may reduce the total strain values. The splitting and inadequate plastic zones during period of back extrusion (step one) may end to the non-uniform deformation. The latter has been already addressed by Nagasekhar et al. [3]. The dead zone formation below the head of inner punch and also at the die corner

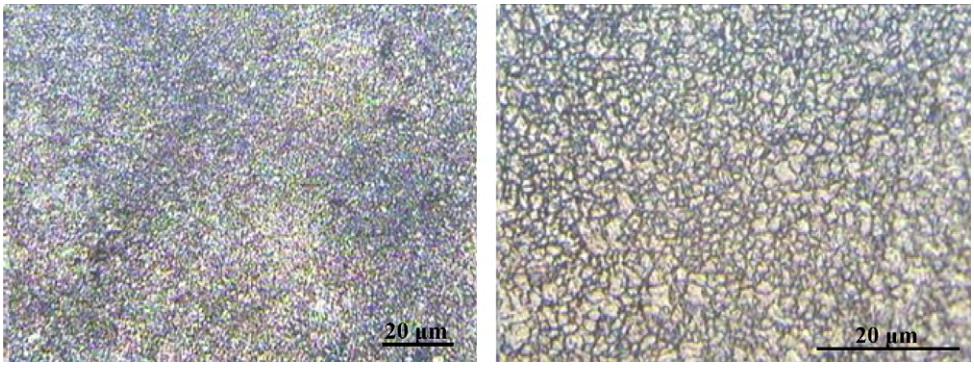

Fig. 9. The typical microstructures of experimental alloy after single pass ABE at 300 °C in two different magnifications.

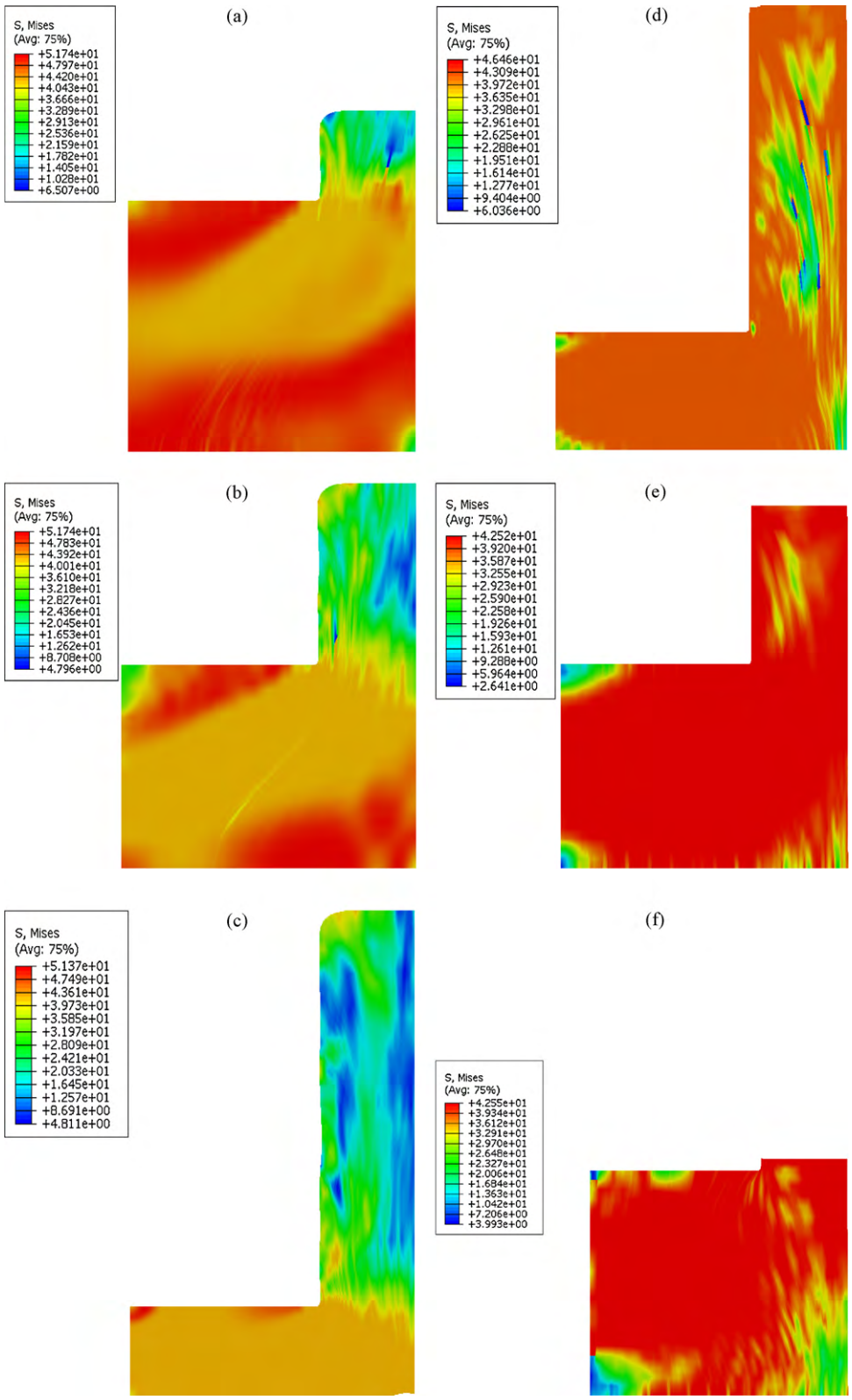

Fig. 10. The effective stress contours for different stages of ABE process, (a, b, c step one and d, e, f step two).

is the major factors accounting for non-uniform strain distribution (strain heterogeneity) throughout the step one. The continuous and comparatively sharp stress contours of plastic zones indicate that the strain homogeneity is achievable during the step two of ABE process.

4. Conclusions

To study the flow pattern and the state of strain during single pass accumulative back extrusion processing of AZ31 magnesium alloy at 300 °C, the three-dimensional FEM simulation and a verifi-

cation procedure through grid method were employed. The results were thoroughly studied by a proper microstructural examination. The conclusions are as follows:

- A deformation channel was formed during step one, the locus of which was displaced as the inner punch proceeds.
- The strain distribution in the cross-section after step one is inhomogeneous, whereas it tends to be reasonably homogenous through applying the second step.
- The results show that the maximum and minimum effective strains are achieved at the inner wall and the bottom of the cup, respectively.
- A homogenous equivalent plastic strain is gained after applying a single pass ABE, whereas the normal strain was inhomogenously distributed.
- After applying a single pass ABE, the amount of obtained EPS was measured to be as high as 4–5. This has not been yet achieved in any other SPD processes after applying a single pass deformation.
- In consistent with FEM results of EPS distribution, a homogenously refined microstructure is observed in AZ31 alloy after ABE processing.
- The strain measurements through grid method present an acceptable conformity with FEM results.
- In contrast to the step one, Von-Mises stress profiles show a continuous and adequate plastic zones obtained during step two. This was believed to assist generating a more homogenous deformation in the entire related cross-section.

References

[1] C. Xu, M. Furukawa, Z. Horita, T.G. Langdon, J. Alloys Compd. 27 (2004) 378.
[2] A. Azushim, R. Kopp, A. Korhonen, D.Y. Yang, F. Micari, G.D. Lahoti, P. Groche, J. Yanagimoto, N. Tsuji, A. Rosochowski, A. Yanagida, CIRP Ann. – Manuf. Technol. 57 (2008) 716.
[3] A.V. Nagasekhar, Y. Tick-Hon, H.P. Seow, J. Mater. Proc. Technol. 192–193 (2007) 449.
[4] M.W. Fu, Y.W. Tham, H.H. Hng, K.B. Lim, Mater. Sci. Eng. A 526 (2009) 84.
[5] Y.W. Tham, M.W. Fu, H.H. Hng, M.S. Yong, K.B. Lim, J. Mater. Proc. Technol. 192–193 (2007) 121.
[6] C.J. Luis-Pérez, R. Luri-Irigoyen, D. Gastón-Ochoa, J. Mater. Proc. Technol. 153–154 (2004) 846.
[7] R. Kocich, M. Greger, M. Kursa, I. Szurman, A. Macháčková, Mater. Sci. Eng. A 527 (2010) 6386.
[8] H.S. Kim, J. Mater. Proc. Technol. 113 (2001) 617.
[9] Y.H. Ji, J.J. Park, W.J. Kim, Mater. Sci. Eng. A 454–455 (2007) 570.
[10] K.-J. Fann, C.-Y. Chen, Key Eng. Mater. 274–276 (2004) 703.
[11] S.M. Fatemi-Varzaneh, A. Zarei-Hanzaki, Mater. Sci. Eng. A 504 (2009) 104.
[12] S.M. Fatemi-Varzaneh, A. Zarei-Hanzaki, 2th UFGNSM, 14–15 Nov., 2009, Tehran, Iran.
[13] S.M. Fatemi-Varzaneh, A. Zarei-Hanzaki, M. Haghshenas, Mater. Sci. Eng. A 497 (2008) 438.
[14] Q.D. Wang, Y.J. Chen, J.B. Lin, L.J. Zhang, C.Q. Zhai, Mater. Lett. 61 (2007) 4599.
[15] D.J. Lee, D.J. Kim, B.M. Kim, J. Mater. Proc. Technol. 139 (2003) 422.
[16] H. Petryk, S. Stupkiewicz, Mater. Sci. Eng. A 444 (2007) 214.